Journal Pre-proof

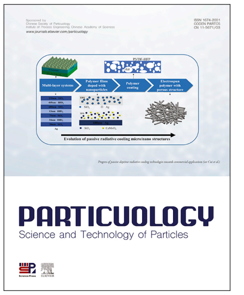

Predicting granule size via in-line NIR spectroscopy during fluidized bed foam granulation and drying

Romain Kersaudy, Maroua Rouabah, Abdoulah Ly, Inès Esma Achouri, Ryan Gosselin, Nicolas Abatzoglou

PII: S1674-2001(25)00278-0

DOI: https://doi.org/10.1016/j.partic.2025.10.011

Reference: PARTIC 2375

To appear in: *Particuology*

Received Date: 17 February 2025

Revised Date: 19 October 2025

Accepted Date: 21 October 2025

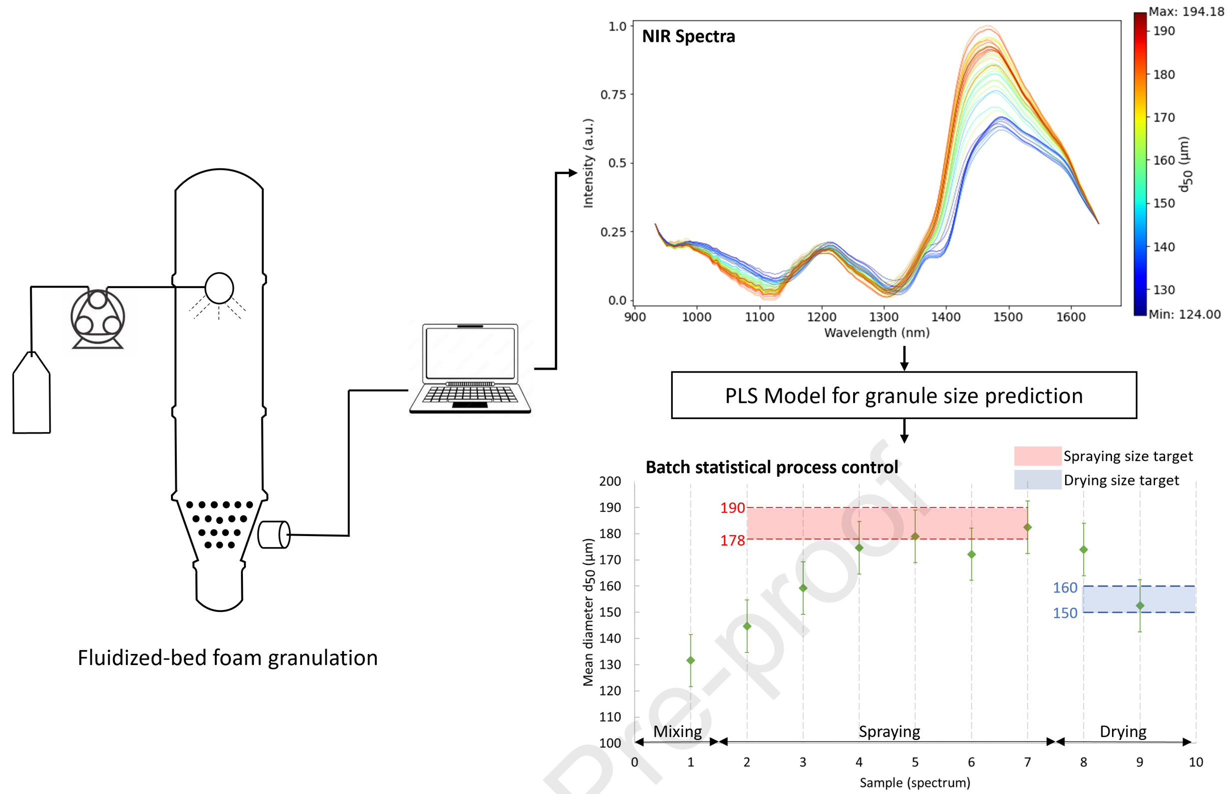

Fluidized-bed foam granulation
NIR Spectra
Intensity (a.u.)
Wavelength (nm)
Max: 194.18
Min: 124.00
d_{50} (µm)
PLS Model for granule size prediction
Batch statistical process control
Spraying size target
Drying size target
Mean diameter d50 (µm)
190
178
160
150
Mixing
Spraying
Drying
Sample (spectrum)

Predicting granule size via in-line NIR spectroscopy during fluidized bed foam granulation and drying

Romain Kersaudy[a], Maroua Rouabah[a*], Abdoulah Ly[b], Inès Esma Achouri[a], Ryan Gosselin[a], Nicolas Abatzoglou[a]

[a] Université de Sherbrooke, GRTP, Sherbrooke, QC, Canada

[b] School of Chemical and Bioprocess Engineering, University College Dublin, Belfield, Dublin 4, Ireland

*Corresponding author. E-mail address: maroua.rouabah@usherbrooke.ca (Maroua Rouabah)

Abstract

Wet granulation-a unit operation involving mixing polymeric binders with powdered formulations-is well established in the pharmaceutical industry, playing a major role in the manufacturing of oral solid dosage forms and improving the physical properties of granules (size, density, shape factor, etc.) before tableting. The foaming properties of aqueous polymeric binders prove useful for binder delivery within the mixing vessel, with foamed binders leading to enhanced process efficiency (binder distribution, drying time, and temperature) and product quality (heat-sensitive components) during granulation. Given the importance of this stage in producing oral solid dosage forms, understanding the relationship between critical process parameters and critical quality attributes is essential. The process analytical technology (PAT) framework enables process design, analysis, and control and facilitates process development via in-line spectroscopy combined with multivariate data analysis to yield critical product information during the unit operation. Herein, we used in-line NIR spectroscopy to monitor granule size in foam granulations of a pharmaceutical compound. The mean granule diameter was predicted using a partial least squares regression (PLSR) model (with a prediction error of 11.8 µm) and combined with a batch statistical process control (BSPC) approach for the temporal monitoring of granule size during three foam granulations.

Keywords: Foam granulation, In-line monitoring, NIR spectroscopy, Size prediction, Batch statistical process control

Nomenclature

d_{50}	Mean particle size, µm
l	Number of wavelengths in the spectral matrix
m	Number of samples (spectra) in test set
n	Number of samples (spectra) in training set
$Q_{v,binder}$	Binder flow rate, g min^{-1}
$Q_{v,air}$	Fluidization air flow rate, Nm^3 h^{-1}
$\hat{y}_i$	Predicted value of interest (here, mean particle diameter predicted by PLSR model, µm)
y_i	Value of interest (here, mean particle diameter, µm)
$\bar{y}$	Average value of the variable of interest (here, average of mean particle diameter, µm)

Abbreviations

BSPC	Batch Statistical Process Control
FDA	Food and Drug Administration
HPMC	Hydroxypropyl Methylcellulose
MCC	Microcrystalline Cellulose
MSPC	Multivariate Statistical Process Control
NIR	Near Infrared
PAT	Process Analytical Technology
PCA	Principal Component Analysis
PC*i*	Principal Component number *i*
PLSR	Partial Least Squares Regression
RMSEC	Root Mean Square Error of Calibration
RMSECV	Root Mean Square Error of Cross Validation
RMSEP	Root Mean Square Error of Prediction
SLS	Sodium Lauryl Sulfate

1. Introduction

1.1 Foam granulation

The wet granulation technique is commonly used in the pharmaceutical industry to enhance the compressibility, cohesion, flowability, and binding properties of powder mixtures, facilitating the formation of suitable granules as an intermediate product in the tableting step (Wang et al., 2022). This method is typically preferred over dry granulation as it produces more uniform mixtures, enhances control over the granule size, and prevents segregation phenomena, thus ensuring greater uniformity in the final dosage form (Arndt et al., 2018).

An unconventional and more recent technique in wet granulation is foam granulation, introduced in the pharmaceutical industry in the early 2000s (Tan & Hapgood, 2012). In this process, foam, rather than traditional liquids, is used as the granulating binder (Tan et al., 2013). The foam is generated by mixing a binder solution with air and then introducing it into the powder bed (Keary & Sheskey, 2004). The bubbles from the foam enhance the solid–liquid contact, and, as they collapse upon contact with powder particles, they facilitate a more uniform distribution of the binder within the powder bed. This promotes agglomeration through capillary forces and the formation of liquid bridges (Jannat et al., 2016; Koo et al., 2024). A significant expected advantage of foam over conventional granulation is a reduction in the required amount of liquid and liquid-to-solid ratio and faster granulation kinetics. Since the binder is dispersed within the foam, it covers a larger surface area, allowing for effective granulation with less liquid (Cantor et al., 2009; Mutch et al., 2019). This minimizes the risk of overwetting and leads to shorter drying times, improving process efficiency; furthermore, the reduced liquid content lowers energy consumption during drying, contributing to more sustainable manufacturing practices. Additionally, foam granulation enhances the quality of granules by enabling better control over the granule size distribution and mechanical strength (Tan & Hapgood, 2011a, 2011b).

This approach can easily be implemented in currently available equipment, such as fluidized bed granulators, with minimal modifications, offering flexibility to pharmaceutical manufacturers seeking to optimize their processes (Thompson, Weatherley, et al., 2012; Thompson, Mu, & Sheskey, 2012).

1.2 Granule size prediction via near infrared spectroscopy

Since the early 2000s, the Food and Drug Administration (FDA) has been encouraging the pharmaceutical industry to optimize manufacturing processes and improve product quality using process analytical technology (PAT) tools and methods. The most widely used analytical technique to date is near infrared (NIR) spectroscopy, given its many advantages over conventional techniques such as liquid or gas chromatography. In NIR spectroscopy, the probe can be inserted directly into the process equipment, allowing for rapid, real-time measurements without the need to withdraw the sample from the process. Historically, this method has been used mainly for its accuracy in monitoring and predicting chemical properties, such as determining the concentrations of pharmaceutical compounds or ensuring quality control of raw materials in different phases (e.g., moisture content in solids; Mainali et al., 2014; Mantanus et al., 2009; Rantanen et al., 2000). However, NIR spectra also contain information about the physical properties of compounds, which can be related to baseline shifts or the presence of offsets. The most commonly referenced method for determining particle size distributions is laser diffraction, which allows for both dry and wet measurements of samples. The use of in-line NIR spectroscopy eliminates the need for sampling and, therefore, avoids various measurement biases, leading to more robust predictive modeling. Many studies have focused on monitoring particle sizes not only due to their importance in predicting the flowability of powders but also because they constitute critical material and quality attributes during the mixing and granulation processes. O’Neil et al. (1998) carried out initial investigations on the offline measurement of the median particle size of compounds, including several powdered drugs and pharmaceutical excipients, such as microcrystalline cellulose (MCC) and lactose monohydrate. They used a two-wavelength multilinear regression model to predict the particle sizes, with an accuracy of 0.17 µm in the 24–406 µm range for MCC and 0.18 µm in the 45–170 µm range for lactose monohydrate. The latter excipient was also studied by Frake et al. (1998) in the early days of offline particle size predictions of pharmaceuticals. Online measurements via NIR spectroscopy were also conducted during this period, specifically by Sekulic et al. (1996), to control the homogeneity of powders in a blender. This spectroscopic technique was later used by Rantanen et al. (2005) to monitor the granulation process and determine the endpoints of high-shear wet granulation in terms of moisture content and granule size. Following their study, a plethora of investigations has been carried out with regard to the real-time monitoring of granule size in wet granulations using multivariate calibration based on partial least squares regression (PLSR; Alcalà et al., 2010; Luukkonen et al., 2008; Nieuwmeyer et al., 2007; Otsuka et al., 2014; Shikata et al., 2017). These studies have been performed in either batch-based high-shear granulation processes or fluidized beds.

Ly et al. (2022) focused on predicting the granule water content during fluidized bed foam granulation (FBFG) and drying using the NIR spectral data gathered in the granulation and drying steps. However, the particle size variations in a given batch and the impact of the process conditions on granule size in this unconventional granulation process are not clearly understood and require further exploration. In the present study, we aimed to monitor the particle sizes of different foam granulation batches in a fluidized bed granulator using a combination of NIR spectroscopy and multivariate data analysis. The predictions were then used in a configuration for the real-time monitoring of granule sizes during both the granulation and drying phases using the batch statistical process control (BSPC) approach.

2. Materials and Methods

2.1 Powder and foam formulation

The formulation used in this study mainly comprised MCC (Vivapur 101®), supplied by JRS Pharma (Patterson, NY, USA), constituting 80% w/w of the mixture. Additionally, the excipients lactose monohydrate, provided by Kerry (Beloit, WI, USA), and sodium croscarmellose (Ac-Di-Sol®) were included at 10% and 5% w/w in the mixture, respectively. Acetaminophen was added as the active pharmaceutical ingredient (API) at a concentration of 5% w/w.

The MCC was pretreated to improve its flowability in the fluidized bed according to a previously established procedure (Ly et al., 2022). In addition, the procedure for preparing the formulation and mixing the various compounds is described in a previous study (Ly et al., 2021).

The binding solution consisted of aqueous hydroxypropyl methylcellulose (HPMC) at varying concentrations, per the experimental design described in Section 2.2. HPMC, acetaminophen, and Ac-Di-Sol® were provided by Pfizer (Montreal, QC, Canada). To decrease the surface tension of the aqueous polymer and increase its foaming ability, sodium lauryl sulfate (SLS), provided by Thermo Fischer Scientific (Tewksbury, MA, USA), was added to the solution.

The foam was generated using an internal air-liquid mixing nozzle, producing a high-quality foam with a gas content of approximately 90-93%, which reflects a high liquid to gas ratio. Regarding the bubble structure, Fig. 1 shows that the bubbles adopt a predominantly polyhedral shape rather than a spherical form of the wet foam. The polyhedral structure enhances the foam’s surface area and stability, while its slow drainage behavior facilitates a more controlled distribution of the binder. The measured drainage rate lies between 0.28 and 0.62 min^{-1}. Furthermore, optical microscopy image shows a lamella thickness between 10 and 13 mm, indicating that the binder layer deposited on each bubble is thin and uniformly distributed. HPMC, acetaminophen, and Ac-Di-Sol® were provided by Pfizer (Montreal, QC, Canada).

Fig. 1

2.2 Experimental design

A total of nine foam granulation runs were performed in a Mini-Glatt fluidized bed granulator-dryer following a two-level fractional factorial (2^{4-1} + 1 central point) experimental design (Table 1). The process parameters in the experimental design involved the binder flow rate, $Q_{v,binder}$ (32 to 38 g/min); the fluidization air flow rate, $Q_{v,air}$ (12 to 16 Nm^3/h); and the HPMC and SLS percentages (0.7 to 1% and 0 to 0.02%, respectively).

Table 1

2.3 Experimental setup

2.3.1 Fluidized bed granulator and dryer

A Mini-Glatt fluidized bed reactor (Glatt, GmbH, Germany) was used in this study, as shown in the experimental setup in Fig. 2. The mixing (heating) and spraying stages were performed at 45 °C for each fluidized bed granulation run. Following the spraying stage, the fluidizing air temperature was increased to 55 °C for the drying step, lasting 12 minutes. Two thermocouples (9 and 10) were positioned at the bottom of the powder container and at the fluidization air outlet to monitor the temperature of the powder. A MicroNIR probe (6) was inserted at the bottom of the container to gather spectral data during the granulation runs. The NIR spectral data and temperature were recorded on a computer using the Viavi MicroNIR Pro Software Suite v2.5.1 and a LabVIEW program, respectively (14). The binding solution was pumped toward the spraying nozzle (4; Spraying System Co., USA) via a peristaltic pump (3). Finally, a pneumatic vibrator (11) was attached to the expansion chamber for all the batches to minimize powder adhesion onto the granulator walls.

Spray nozzles used in fluidized bed granulation are typically bi-fluid atomizers with external mixing. In this configuration, the contact point between the two fluids is at the nozzle's tip. The ¼ JAC spray nozzle setup used in these experiments included an air cap (PA67-6-20-70) and a fluid cap (PF1650) from Spraying Systems Co. (Wheaton, USA): air and the binding solution are mixed within a chamber before the tip, with the mixed fluids exiting as foam through six holes. A pressure of 5 kPa was required to produce foam with this nozzle.

Using a fluidized bed causes powder particles to build up at the nozzle tip, which can then interfere with the homogeneous and continuous generation of foam. Therefore, during foam delivery to the powder bed, fluidization was interrupted for approximately 10 seconds, during which time the atomization pressure was set to 5 kPa. After dispensing the foam, the fluidization pressure was increased to 100 kPa for 52 seconds to fluidize the wet particles and minimize particle buildup on the nozzle. The entire process was automated using the instrument’s software to ensure greater accuracy and good reproducibility.

Fig. 2

2.3.2 NIR spectroscopy

The MicroNIR probe (Viavi Solutions) was mounted in the powder container of the granulator vessel. The spectra were then measured over the range of 908.1–1676.2 nm, with a resolution of 6.2 nm (integration time = 14.6 ms, and number of scans = 100), during the three phases of mixing, spraying, and drying. Each spectrum was measured in triplicate and then averaged, resulting in a total of 72 spectra for the 9 foam granulation runs.

2.4 Granule size distribution

Granules were sampled for each spectrum, and the particle size distribution was determined using a Malvern Panalytical Mastersizer 3000. The measurement parameters included an air pressure setting of 1.1 barg (110 kPa), a vibration rate of 50%, and a hopper gap of 1.5 mm to prevent the activation of the granule breaking mechanism. The particle size analysis was conducted using Mie scattering theory with a standard analysis protocol, assuming a particle refractive index of 1.652 and a laser obscuration value of 0.99%. Ten measurements were taken and averaged for each sample, and the mean diameter (d_{50}) was then kept as a size descriptor for the subsequent multivariate data analysis.

Fig. 3 displays the particle size distributions by volume of six samples taken from granulation batch No. 5, color-coded according to the granulation stages: mixing, spraying, and drying. The curves indicate the percentage by volume of particles (volume density) measured in each size class on a logarithmic scale.

The figure shows a clear increase in particle size during the granulation process following foam binder addition. This reflects the rapid and uniform dispersion of the foam across the powder bed, which promotes simultaneous wetting and growth, consistent with the mechanical dispersion regime described for foam granulation (Tan et al., 2013; Tan and Hapgood, 2011b, 2011a).

A slight narrowing of the particle size distribution is observed during the drying phase (average span of 1.79 compared to 1.80 for the spraying phase). This could be attributed to attrition and breakage phenomenon, which are likely to be more pronounced during the drying phase as particles become drier and more fragile (De Leersnyder et al., 2018).

A population of fines is observed during the mixing phase which then decreases during spraying and drying stages. At present, no sieve assay data are available to directly quantify the evolution of fine, intermediate, and coarse fractions during the three stages. Future work combining NIR moisture monitoring with sieve fraction analysis is planned to investigate the mechanisms responsible for the post-binder narrowing of the PSD in foam-based granulation.

Although sieve data are not currently available, fines and large agglomerates were explicitly included in the modeling approach to enhance its robustness. These agglomerates can form temporarily and then disintegrate under fluidization, particularly during drying, reflecting the inherent dynamics of the process. Cumulative distribution analysis showed that particles larger than 976 µm represent a negligible fraction of the sample (e.g., less than 3% in batch No. 5). They were nevertheless retained in the analysis to better capture the intrinsic variability of the process.

Other characteristics, such as the shape and morphology of particles and pregranulated material, the surface tension and viscosity of the binding solution, and foam quality and stability, have been described in previous work (Ly et al., 2022).

Fig. 3

2.5 Chemometrics

NIR spectra are notably complex due to the overlapping of different bands characteristic of the molecular vibrational modes of the analyzed compounds. Their visual interpretation is, therefore, not viable; statistical methods (chemometrics) are, thus, required to extract the greatest amount of physicochemical information possible on the medium under study (Mark, 1989).

Data analysis and processing were conducted using Python 3.11. The scikit-learn (Pedregosa et al., 2011), chemotools ("Chemotools: Package to integrate chemometrics in scikit-learn pipelines", n.d.), and RG ("RG: Ryan's go-to Python functions", n.d.) libraries were utilized for the implementation of machine learning algorithms and data manipulation.

2.5.1 Spectral preprocessing

In most instances, NIR spectra are preprocessed to eliminate the additive and/or multiplicative effects caused by the physicochemical aspects of the analyzed sample. This study focuses on the prediction of particle size; in this way, the spectral information of interest is directly related to the physical effects that cause the offset to vary as a function of the path length of the infrared beam. In our case, it is, therefore, inappropriate to employ common preprocessing techniques such as normalization or derivatives that reduce this feature. Considering this, the preprocessing measures applied to these data involved a reduction in the wavelength range (from 908.1–1676.2 nm to 932.8–1645.2 nm) of the spectra to increase the precision at the extremities of the detector range, mean centering, and a baseline correction. Fig. 4 displays the preprocessed spectra from the training set, colored according to their corresponding mean particle diameter.

Fig. 4

2.5.2 Multivariate data analysis

Principal component analysis (PCA) is the most widely used multivariate method for data exploration. It involves compressing the initial highly correlated data into several orthogonal principal components that explain the maximum variability in the spectra (Hotelling, 1933). This analysis yields several interpretable results regarding how samples and variables are related to the principal components: scores representing the new coordinates of each sample (projection of the samples) in the new space defined by the calculated principal components; and loading spectra, representing the most important spectral bands and their relative contribution to each principal component. These data are usually represented graphically, facilitating their interpretation.

PCA decomposition was applied to the preprocessed spectral data ($n \times l$: 72×116) to observe the relevant characteristics and detect any outliers that might reduce the performance of the particle size prediction model. The presence of outliers was assessed using the score plot; this represents the data in the space defined by the first two principal components, t_1 and t_2 in Fig. 5, which explain 96.25 and 2.09% of the total spectral variance, respectively. Each point in this figure corresponds to a sample (spectrum) and is colored according to the granulation stage at which it was measured, that is, the mixing (M), spraying (S), and drying (D) stages. Firstly, there are no clusters of samples corresponding to the pelleting steps, indicating that the measured NIR spectra are relatively close to each other. Secondly, a few points lie outside the 95% confidence interval, though they are not considered outliers since these spectra are similar to the rest of the data. Consequently, all spectra were kept for the remainder of the data analysis.

PLSR is the most widespread regression method used in spectral data analysis to create empirical models for quantifying one or more parameters from linear data; this technique was used to develop the particle size quantification model herein. The principle is the same as in PCA, where the data are reduced to orthogonal principal components, also known as latent variables. The only difference is that a Y matrix, containing the reference value of the parameter to be predicted, is added to the X matrix of the spectra, and latent variables are calculated to model the covariance between these two spaces (Geladi & Kowalski, 1986). In our case, the Y matrix contains the reference values for the particle sizes. Further, the mean diameter (d_{50}), evaluated from the particle size distribution measurements, was selected in this study.

Prior to the statistical analysis, the spectra were randomly split into training and test sets in a 0.7/0.3 ratio, resulting in a training set of 50 spectra and a test set of 22 spectra. Additionally, k-fold cross-validation was used to validate the calibration model (built from the training set) with 10 randomized folds.

In building a PLSR model, it is crucial to choose an appropriate number of latent variables to ensure the robustness of the model for future predictions while avoiding underfitting or overfitting. The optimal number of latent variables was selected using cross-validation and assessing the obtained model performance after each loop via the root mean square error of cross validation (RMSECV), calculated as in Equation 1:

$$RMSECV = \sqrt{\frac{1}{n}\sum_{i=1}^{n}(\hat{y}_{i} - y_{i})^{2}}\ , \qquad (1)$$

where n is the number of samples in the training set, $\hat{y}_i$ is the mean particle diameter (d_{50}) predicted by the PLSR model, and y_i is the mean granule diameter (d50) obtained via the referenced method for sample i.

External validation of the model was performed with the test set. The global performance of the model was evaluated by calculating the R^2 and root mean square error of prediction (RMSEP) values, as in Equations 2 and 3:

$$R^2 = 1 - \frac{\sum_{i=1}^{n\ or\ m}(y_{i} - \hat{y}_{i})^2}{\sum_{i=1}^{n\ or\ m}(y_{i} - \bar{y})^2} \qquad (2)$$

$$RMSEP = \sqrt{\frac{1}{m}\sum_{i=1}^{n}(\hat{y}_{i} - y_{i})^{2}}\ , \qquad (3)$$

where m is the number of samples in the test set, and $\bar{y}$ is the overall average of d_{50} reference values.

Fig. 5

3. Results and Discussion

3.1 PCA unsupervised monitoring-batch statistical process control (BSPC)

PCA is a powerful tool that, in addition to data mining, classification, or outlier detection, can be used in a BSPC approach for batch process control. This approach was used to explore the NIR spectral data acquired in the nine foam granulation runs performed herein. Typically, the principal component scores for different batches are plotted, and their evolution over time is then analyzed. Fig. 6 shows the time evolution of the scores of the first principal component (PC1) for the nine batches; each point represents a spectrum acquired during each of the 9 batches performed; this process is reasonable as t_1 explains 96.25% of the variance. The same trend can be noted for each foam granulation. The plot in this figure indicates different phases for each batch: an initial phase, during which the PC1 scores rise, and a second phase, during which these scores decline. By relating these observations to the particle size distribution measurements and the granulation phases, one can note that the increase in the scores correlates with the increase in particle size during the first two phases of granulation-mixing and spraying. The second phase correlates with the decrease in particle size during the drying phase (Fig. 7). These observations suggest a relationship between the spectral data and the size of the granules circulating in the fluidized bed. It is, therefore, beneficial to use this spectral and physical information to build a model for predicting granule size based on the NIR spectra.

Fig. 6, 7

3.2 Granule size prediction

The spectral database was randomly divided into training and test sets in a 0.7/0.3 ratio, yielding 50 spectra for the training set and 22 spectra for the test set. A PLSR model was then built from the training dataset. Only one latent variable was considered, yielding an explained variance close to 80%. Fig. 8 shows the predictions of the mean granule diameter using the NIR spectra and PLSR for the calibration and validation datasets. The root mean square error of calibration (RMSEC) is 8.7 μm and the RMSECV is 9.0 μm for the calibration samples, indicating the model's relatively accurate prediction of the mean granule diameter. The mean granule size of two calibration samples appears to be underestimated (the points furthest to the right of the blue line in this figure). These calibration points were not considered outliers, given the strong similarity of the spectra to the rest of the data and the mean diameter in the investigated range. The RMSEP obtained from the prediction of the external validation dataset is approximately 11.8 μm. Overall, the prediction error mostly arises from samples at the extreme points of the size range analyzed herein. The small number of values at the smallest sizes (less than 130 μm) and the largest sizes (greater than 190 μm) does not provide the one-component PLSR model with sufficient information to guarantee accurate and reliable predictions at extreme sizes. Nevertheless, the PLSR model calculated from the available data remains satisfactory for our application and provides useful information on the mean diameter of the granules in the fluidized bed. The granule size specifications for this application have been set between 150 and 190 μm; thus, a model that yields accurate predictions in this range is sufficient. However, samples of smaller or larger sizes are retained to incorporate the related information into the model and better anticipate deviations in the foam granulation process.

Fig. 8

3.3 Batch statistical process control

From an industrial perspective, monitoring critical process parameters is essential. Part of the PAT approach is concerned with this aspect and aims to use the information available on the processes from previously installed sensors (temperature, pressure, flow rate, etc.) or more complex sensors involving, for example, optical and vibrational spectroscopy. Process monitoring involves noting any anomalies or deviations in the process in real time using control charts. Multivariate statistical process control (MSPC) aims to use data predicted by multivariate models in cases where no univariate sensor is present to predict a specific parameter; for example, a PLSR model can be used to predict a chemical or physical characteristic in a process from spectra acquired via a spectroscopic technique. Control charts are then used to track the parameter in question over time (Nomikos & MacGregor, 1995). The term "BSPC" is used to refer to processes that do not run continuously but rather in batch mode. In the final stages of the study, we used predictions of the mean granule diameter from the MicroNIR-spectroscopy-based PLSR model for the BSPC approach. For this application, mean diameter targets were set for each of the spraying and drying stages to meet the product specifications. The first target was set to values between 178 and 190 µm at the end of the spraying stage. Once this target had been achieved, the drying stage could be started. Drying was then completed when the mean granule diameter fell between 150 and 160 µm. Fig. 9 shows the evolution of the predicted mean diameter over the course of three foam granulations. The green data points represent mean diameter predictions, with the error bar corresponding to the RMSEP of the PLSR model. In the first batch, in-line monitoring reveals that the mean diameter achieved at the end of the drying stage is insufficient (167 µm). Using the MicroNIR probe, drying should have continued to reach the target size range. Conversely, in the second batch, the final prediction reveals a mean diameter of 140 µm, which is significantly low compared to the specifications. The granules had, therefore, been overdried, and the drying stage should have been ended earlier. Finally, in the third batch, the specifications were all met at the end of both the spraying and drying stages. This demonstrates the value of the BSPC approach for monitoring the notably critical parameter of particle size using a MicroNIR spectroscopic probe. This approach allows for improved monitoring and more precise process control, increasing productivity and reducing the maintenance costs associated with the various anomalies in the production line caused by nonideal particle sizes.

Fig. 9

3.4 Optimal parameter search

The research project's objective of optimizing the granulation process was pursued, with the aim of determining the optimal parameters to ensure that the mean diameter criterion, d50, of the granules at the completion of the granulation process was between 150 and 160 µm, while also attaining the most narrowly distributed particle size distribution possible. In the latter case, the span defined as a dimensionless parameter representing the width of the distribution, as given by the formula (d90-d10)/d50, was chosen. The search for the optimal parameters among those explored during the nine granulation batches of this study was carried out using Design Expert® (Stat-Ease, Inc) statistical software. The response criteria that were selected were therefore such that they would comply with a final mean diameter d50 between 150 and 160 µm, whilst minimizing the span value.

The optimal parameters required to achieve these targets are outlined in Fig. 10, showing good confidence in the results with a desirability of 0.99. In order to obtain granules with a mean diameter of 160 µm and a span of 1.421 (the minimum obtained during the experiments) the following process parameters are to be used: a binder flow rate of 38 g/min, an air flow rate of 14.4 Nm^3/h, a binder content (HPMC) of 0.7% and a surfactant content (SLS) of 0.02%.

It is interesting to note that the best results were obtained with the highest binder flow rate and lowest binder content resulting in a short binder addition time. In foam granulation, the binder distribution is governed by mechanical dispersion of a high void foam through the powder bed, rather than by droplet impact and penetration. By distributing foam quickly while maintaining a low binder concentration, local liquid saturation is kept low and the process is maintained in the mechanical dispersion regime, which leads to more uniform and simultaneous nucleation, preventing overwetting and coalescence. (Tan et al., 2013; Tan and Hapgood, 2011a, 2011b) show that high foam quality and short addition times favor narrow granule size distributions, while longer additions lead to a drainage-controlled growth and wider distributions

Furthermore, foam granulation produces finer and more homogeneous granules than spray (Mutch et al., 2019), confirming the distinct wetting mechanism underlying this optimum.

Fig. 10

4. Conclusions

NIR spectroscopy was used herein for the in-line monitoring of the granule size during foam granulations of a pharmaceutical formulation within a fluidized bed reactor. Batch foam granulations were performed, varying the binder and fluidization air flow rates and the concentrations of HPMC and SLS used in the binder solution. The NIR data recorded during the three granulation phases-mixing, spraying, and drying-were linked to the mean granule diameter of the samples to build a PLSR model. A model with one latent variable gave predictions with an RMSEP of 11.8 μm. The PLSR predictions were then combined with a BSPC approach to monitor process evolution and control the granule size in the different stages of the foam granulations. In-line measurements via NIR spectroscopy have been proven beneficial, providing critical information in a PAT approach for a process widely used in the pharmaceutical industry. This probe format offers greater flexibility and ease of scale-up while also maintaining a notably high analytical performance. The combination of NIR spectroscopy and particle size monitoring using a statistical process control approach represents a significant advancement in understanding and controlling complex processes such as fluidized bed granulation.

Acknowledgments

The authors are indebted to NSERC Canada and Pfizer Canada for funding related to this work. The technical and scientific contributions of GRTP's personnel and, more specifically, Elisabeth Perreault, Jacques Gagné, and Marc Couture are gratefully acknowledged.

References

Alcalà, M., Blanco, M., Bautista, M., & González, J. M. (2010). On-line monitoring of a granulation process by NIR spectroscopy. *J. Pharm. Sci.*, *99*(1), 336–345. https://doi.org/10.1002/jps.21818

Arndt, O.-R., Baggio, R., Adam, A. K., Harting, J., Franceschinis, E., & Kleinebudde, P. (2018). Impact of different dry and wet granulation techniques on granule and tablet properties: A comparative study. *J. Pharm. Sci.*, *107*(12), 3143–3152. https://doi.org/10.1016/j.xphs.2018.09.006

Cantor, S. L., Kothari, S., & Koo, O. M. Y. (2009). Evaluation of the physical and mechanical properties of high drug load formulations: Wet granulation vs. novel foam granulation. *Powder Technol.*, *195*(1), 15–24. https://doi.org/10.1016/j.powtec.2009.05.003

Chemotools: Package to integrate chemometrics in scikit-learn pipelines [OS Independent]. (n.d.). Python. Retrieved December 3, 2024, from https://github.com/paucablop/chemotools

De Leersnyder, F., Vanhoorne, V., Bekaert, H., Vercruysse, J., Ghijs, M., Bostijn, N., Verstraeten, M., Cappuyns, P., Van Assche, I., Vander Heyden, Y., Ziemons, E., Remon, J.P., Nopens, I., Vervaet, C., De Beer, T., 2018. Breakage and drying behaviour of granules in a continuous fluid bed dryer: Influence of process parameters and wet granule transfer. European Journal of Pharmaceutical Sciences 115, 223–232. https://doi.org/10.1016/j.ejps.2018.01.037

Frake, P., Luscombe, C. N., Rudd, D. R., Gill, I., Waterhouse, J., Frake, P., & Jayasooriya, U. A. (1998). Near-infrared mass median particle size determination of lactose monohydrate, evaluating several chemometric approaches. *The Analyst*, *123*(10), 2043–2046. https://doi.org/10.1039/a802532k

Geladi, P., & Kowalski, B. R. (1986). Partial least-squares regression: A tutorial. *Anal. Chim. Acta*, *185*, 1–17. https://doi.org/10.1016/0003-2670(86)80028-9

Hotelling, H. (1933). Analysis of a complex of statistical variables into principal components. *J. Educ. Psychol.*, *24*(6), 417–441. https://doi.org/10.1037/h0071325

Jannat, E., Arif, A. A., Hasan, M. M., Zarziz, A. B., & Rashid, H. A. (2016). Granulation techniques & its updated modules. *Pharma Innov.*, *5*(10), 134–141.

Keary, C. M., & Sheskey, P. J. (2004). Preliminary report of the discovery of a new pharmaceutical granulation process using foamed aqueous binders.

Koo, O., Patel, C., & Nikfar, F. (2024). Effect of hydroxy propyl cellulose grade and foam quality on foam granulation of a high drug load formulation. *Int. J. Pharm.*, *657*, 124171. https://doi.org/10.1016/j.ijpharm.2024.124171

Luukkonen, P., Fransson, M., Björn, I. N., Hautala, J., Lagerholm, B., & Folestad, S. (2008). Real-time assessment of granule and tablet properties using in-line data from a high-shear granulation process. *J. Pharm. Sci.*, *97*(2), 950–959. https://doi.org/10.1002/jps.20998

Ly, A., Achouri, I. E., Gosselin, R., & Abatzoglou, N. (2021). Wet granulation end point prediction using dimensionless numbers in a mixer torque rheometer: Relationship between capillary and Weber numbers and the optimal wet mass consistency. *Int. J. Pharm.*, *605*, 120823. https://doi.org/10.1016/j.ijpharm.2021.120823

Ly, A., Achouri, I. E., Gosselin, R., & Abatzoglou, N. (2022). Sequential fixed-fluidized bed foam granulation (SFFBFG) and drying: Multivariate model development for water content monitoring with near–infrared spectroscopy. *Chem. Eng. Sci.*, *262*, 118039. https://doi.org/10.1016/j.ces.2022.118039

Mainali, D., Li, J., Yehl, P., & Chetwyn, N. (2014). Development of a comprehensive near infrared spectroscopy calibration model for rapid measurements of moisture content in multiple pharmaceutical products. *J. Pharm. Biomed. Anal.*, *95*, 169–175. https://doi.org/10.1016/j.jpba.2014.03.001

Mantanus, J., Ziémons, E., Lebrun, P., Rozet, E., Klinkenberg, R., Streel, B., Evrard, B., & Hubert, Ph. (2009). Moisture content determination of pharmaceutical pellets by near infrared spectroscopy: Method development and validation. *Anal. Chim. Acta*, *642*(1), 186–192. https://doi.org/10.1016/j.aca.2008.12.031

Mark, H. (1989). Chemometrics in near-infrared spectroscopy. *Anal. Chim. Acta*, *223*, 75–93. https://doi.org/10.1016/S0003-2670(00)84075-1

Mutch, G. A., Hapgood, K. P., Shen, R., & Selomulya, C. (2019). An investigation on the dissolution qualities of foam granulated products. *Powder Technol.*, *343*, 693–704. https://doi.org/10.1016/j.powtec.2018.11.086

Nieuwmeyer, F. J. S., Damen, M., Gerich, A., Rusmini, F., van der Voort Maarschalk, K., & Vromans, H. (2007). Granule characterization during fluid bed drying by development of a near infrared method to determine water content and median granule size. *Pharm. Res.*, *24*(10), 1854–1861. https://doi.org/10.1007/s11095-007-9305-5

Nomikos, P., & MacGregor, J. F. (1995). Multivariate SPC charts for monitoring batch processes. *Technometrics*, *37*(1), 41–59. https://doi.org/10.1080/00401706.1995.10485888

O'Neil, A. J., Jee, R. D., & Moffat, A. C. (1998). The application of multiple linear regression to the measurement of the median particle size of drugs and pharmaceutical excipients by near-infrared spectroscopy. *Analyst*, *123*(11), 2297–2302. https://doi.org/10.1039/A806001K

Otsuka, M., Koyama, A., & Hattori, Y. (2014). Real-time release monitoring for water content and mean particle size of granules in lab-sized fluid-bed granulator by near-infrared spectroscopy. *RSC Adv.*, *4*(34), 17461–17468. https://doi.org/10.1039/C3RA45375H

Pedregosa, F., Varoquaux, G., Gramfort, A., Michel, V., Thirion, B., Grisel, O., Blondel, M., Prettenhofer, P., Weiss, R., Dubourg, V., Vanderplas, J., Passos, A., Cournapeau, D., Brucher, M., Perrot, M., & Duchesnay, É. (2011). Scikit-learn: Machine learning in Python. *J. Mach. Learn. Res.*, *12*(85), 2825–2830.

Rantanen, J., Antikainen, O., Mannermaa, J.-P., & Yliruusi, J. (2000). Use of the near-infrared reflectance method for measurement of moisture content during granulation. *Pharm. Dev. Technol.*, *5*(2), 209–217. https://doi.org/10.1081/PDT-100100536

Rantanen, J., Wikström, H., Turner, R., & Taylor, L. S. (2005). Use of in-line near-infrared spectroscopy in combination with chemometrics for improved understanding of pharmaceutical processes. *Anal. Chem.*, *77*(2), 556–563. https://doi.org/10.1021/ac048842u

RG: Ryan's go-to Python functions [OS Independent]. (n.d.). Python. Retrieved December 3, 2024, from https://www.usherbrooke.ca/gchimiquebiotech/departement/professeurs/ryan-gosselin/

Sekulic, S. S., Ward, H. W., Brannegan, D. R., Stanley, E. D., Evans, C. L., Sciavolino, S. T., Hailey, P. A., & Aldridge, P. K. (1996). On-line monitoring of powder blend homogeneity by near-infrared spectroscopy. *Anal. Chem.*, *68*(3), 509–513. https://doi.org/10.1021/ac950964m

Shikata, F., Kimura, S., Hattori, Y., & Otsuka, M. (2017). Real-time monitoring of granule properties during high shear wet granulation by near-infrared spectroscopy with a chemometrics approach. *RSC Adv.*, *7*(61), 38307–38317. https://doi.org/10.1039/C7RA05252A

Tan, M. X. L., & Hapgood, K. P. (2011a). Foam granulation: Liquid penetration or mechanical dispersion? *Chem. Eng. Sci.*, *66*(21), 5204–5211. https://doi.org/10.1016/j.ces.2011.07.012

Tan, M. X. L., & Hapgood, K. P. (2011b). Foam granulation: Binder dispersion and nucleation in mixer-granulators. *Chem. Eng. Res. Des.*, *89*(5), 526–536. https://doi.org/10.1016/j.cherd.2010.07.001

Tan, M. X. L., & Hapgood, K. P. (2012). Foam granulation: Effects of formulation and process conditions on granule size distributions. *Powder Technol.*, *218*, 149–156. https://doi.org/10.1016/j.powtec.2011.12.006

Tan, M. X. L., Nguyen, T. H., & Hapgood, K. P. (2013). Drug distribution in wet granulation: Foam versus spray.

Thompson, M. R., Mu, B., & Sheskey, P. J. (2012). Aspects of foam stability influencing foam granulation in a twin screw extruder. *Powder Technol.*, *228*, 339–348. https://doi.org/10.1016/j.powtec.2012.05.050

Thompson, M. R., Weatherley, S., Pukadyil, R. N., & Sheskey, P. J. (2012). Foam granulation: New developments in pharmaceutical solid oral dosage forms using twin screw extrusion machinery. *Drug Dev. Ind. Pharm.*, *38*(7), 771–784. https://doi.org/10.3109/03639045.2011.633265

Wang, B., Sun, X., Xiang, J., Guo, X., Cheng, Z., Liu, W., & Tan, S. (2022). A critical review on granulation of pharmaceuticals and excipients: Principle, analysis and typical applications. *Powder Technol.*, *401*, 117329. https://doi.org/10.1016/j.powtec.2022.117329

Predicting granule size via in-line NIR spectroscopy during fluidized bed foam granulation and drying

Romain Kersaudy[a], Maroua Rouabah[a*], Abdoulah Ly[b], Inès Esma Achouri[a], Ryan Gosselin[a], Nicolas Abatzoglou[a]

Fig captions:

Fig. 1. Optical microscopy image of 0.7% aqueous HPMC foam showing lamella and bubble size.

Fig. 2. Experimental setup of the fluidized bed granulator: (1) air compressor, (2) binder solution container, (3) peristaltic pump, (4) internal mixing nozzle, (5) powder bed, (6) NIR probe, (7) heater, (8) air exhaust, (9) and (10) thermocouples, (11) vibrator, (12) data acquisitors, (13) low/high-pressure regulator setup, and (14) computer.

Fig. 3. Particle size distribution of six samples taken during granulation No. 5: mixing (blue), spraying (green), and drying (red) stages.

Fig. 4. Preprocessed training set NIR spectra (variable selection and baseline correction), colored according to the mean particle diameter (d_{50}).

Fig. 5. Score plot of t_2 versus t_1 of the spectra, colored according to the granulation step: drying (D), mixing (M), and spraying (S).

Fig. 6. PCA score plot of the first principal component (PC1) of the nine granulation batches.

Fig. 7. Evolution of PC1 scores and mean granule diameter (d_{50}) in granulation batch No. 5, showing the corresponding granulation stages.

Fig. 8. Mean granule diameter (d_{50}) predicted via PLSR model versus measured mean particle diameter.

Fig. 9. BSPC of mean granule diameter predicted by the PLSR model during three foam granulation trials: Nos. 1, 2, and 3.

Fig. 10. Results of the optimal parameter search from Design Expert.

Predicting granule size via in-line NIR spectroscopy during fluidized bed foam granulation and drying

Romain Kersaudy[a], Maroua Rouabah[a*], Abdoulah Ly[b], Inès Esma Achouri[a], Ryan Gosselin[a], Nicolas Abatzoglou[a]

Table:

Table 1 Two-level fractional factorial experimental design.

Batch No.	$Q_{v,binder}$ (g/min)	$Q_{v,air}$ (Nm^3/h)	HPMC (%)	SLS (%)
1	32	12	0.7	0
2	32	16	1	0
3	32	16	0.7	0.02
4	32	12	1	0.02
5	38	16	0.7	0
6	38	12	1	0
7	38	12	0.7	0.02
8	38	16	1	0.02
9	35	14	0.85	0.01

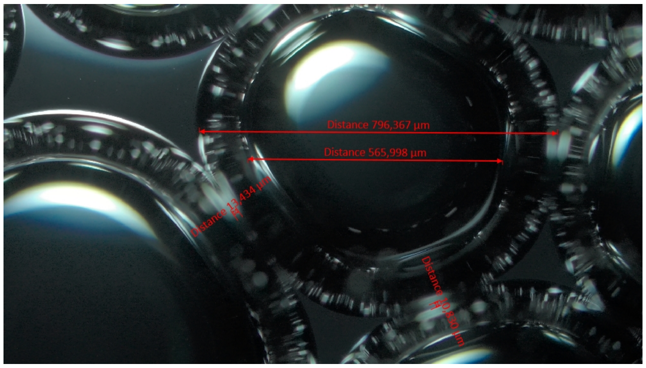
Distance 796,367 µm
Distance 565,998 µm
Distance 13,434 µm
Distance 10,830 µm

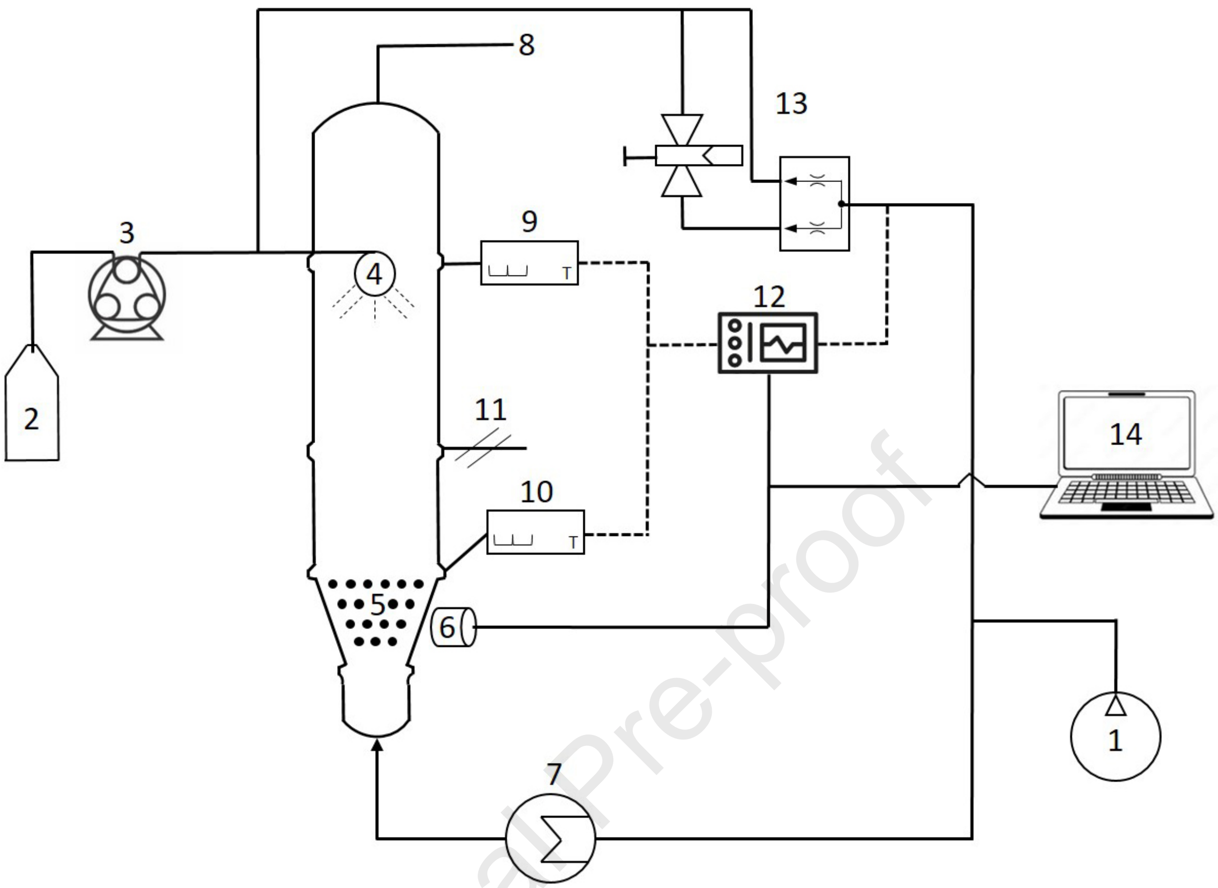

8
13
3
9
4
12
2
11
14
10
5
6
1
7

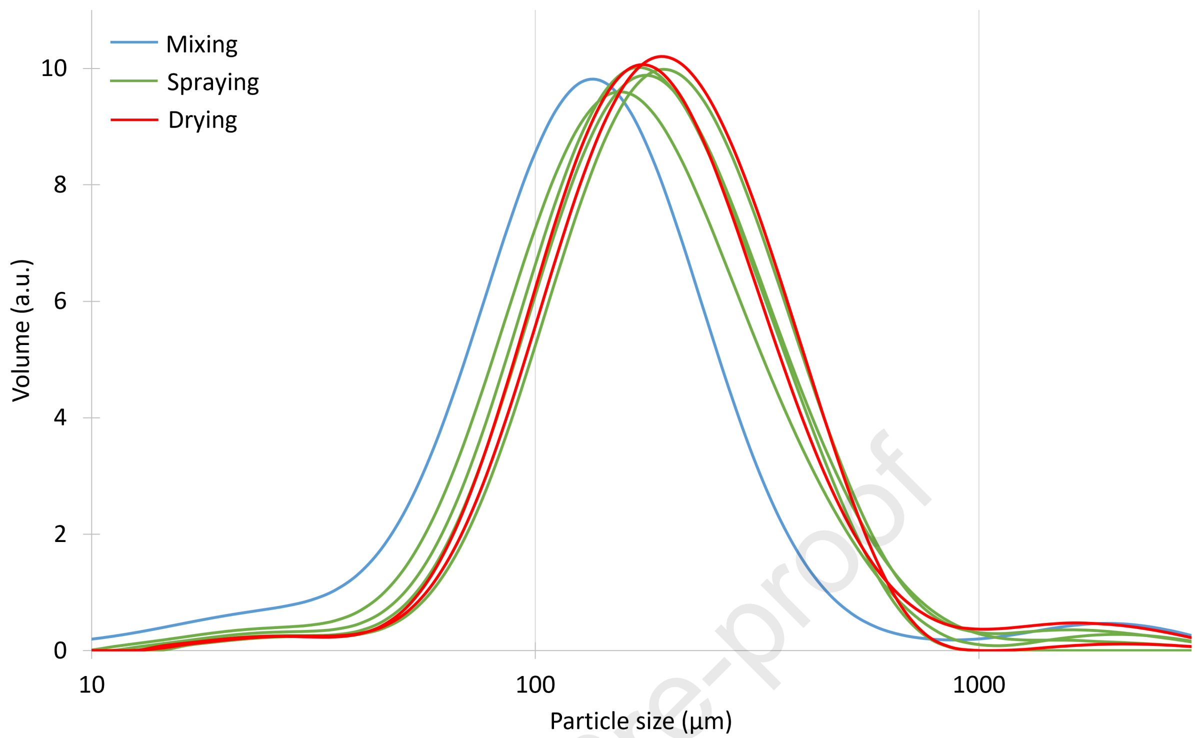
Mixing
Spraying
Drying
Volume (a.u.)
0
2
4
6
8
10
10
100
1000
Particle size (µm)

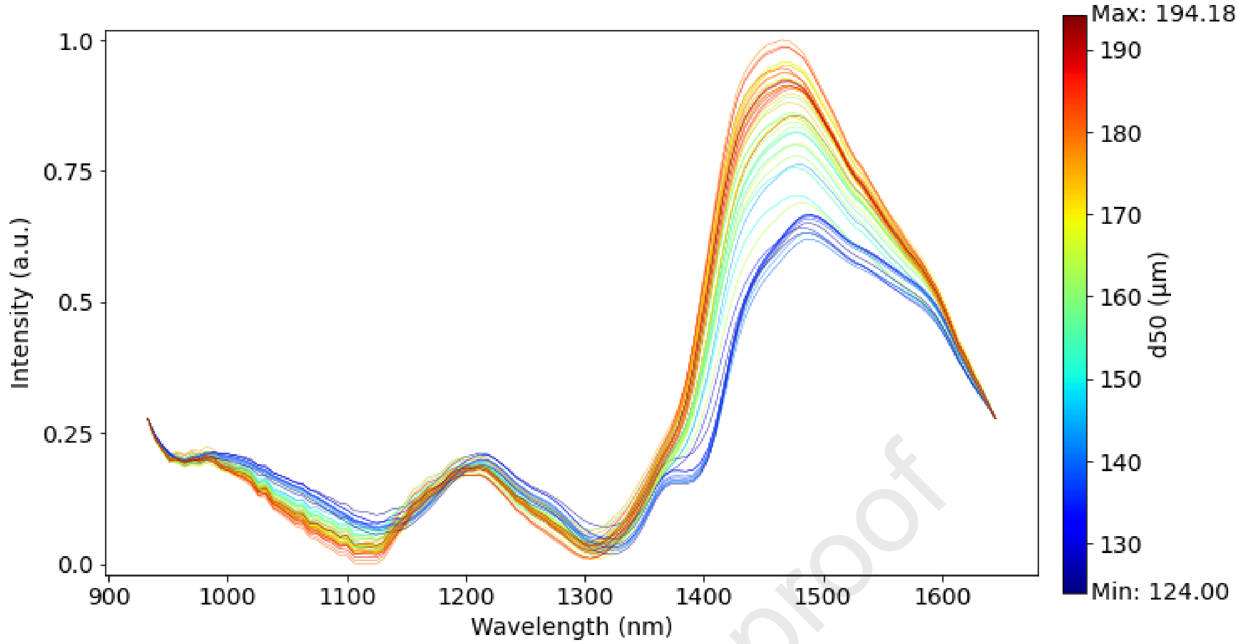

Intensity (a.u.)
1.0
0.75
0.5
0.25
0.0
900
1000
1100
1200
1300
1400
1500
1600
Wavelength (nm)
Max: 194.18
190
180
170
160
150
140
130
Min: 124.00
d50 (µm)

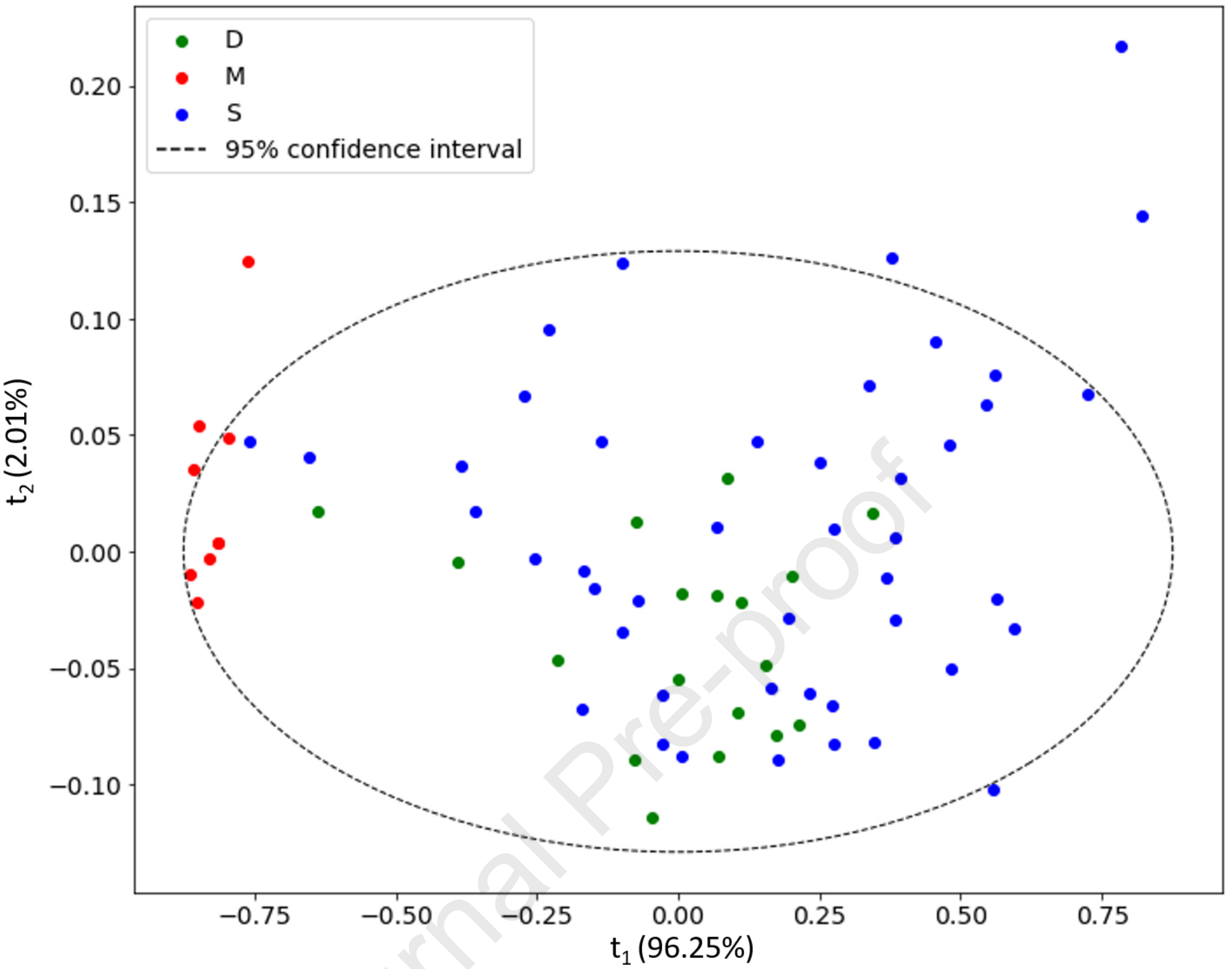
D
M
S
95% confidence interval
0.20
0.15
0.10
0.05
0.00
−0.05
−0.10
−0.75
−0.50
−0.25
0.00
0.25
0.50
0.75
t_2 (2.01%)
t_1 (96.25%)

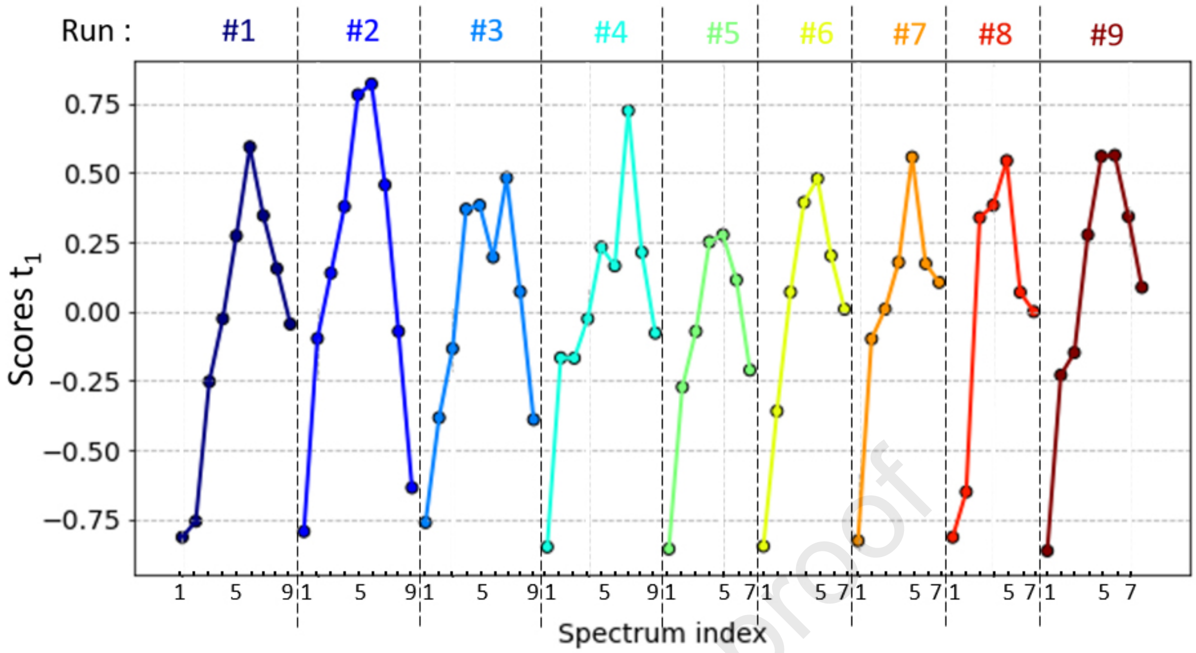
Run :
#1
#2
#3
#4
#5
#6
#7
#8
#9
0.75
0.50
0.25
0.00
−0.25
−0.50
−0.75
Scores t_1
1 5 9
1 5 9
1 5 9
1 5 9
1 5 7
1 5 7
1 5 7
1 5 7
1 5 7
Spectrum index

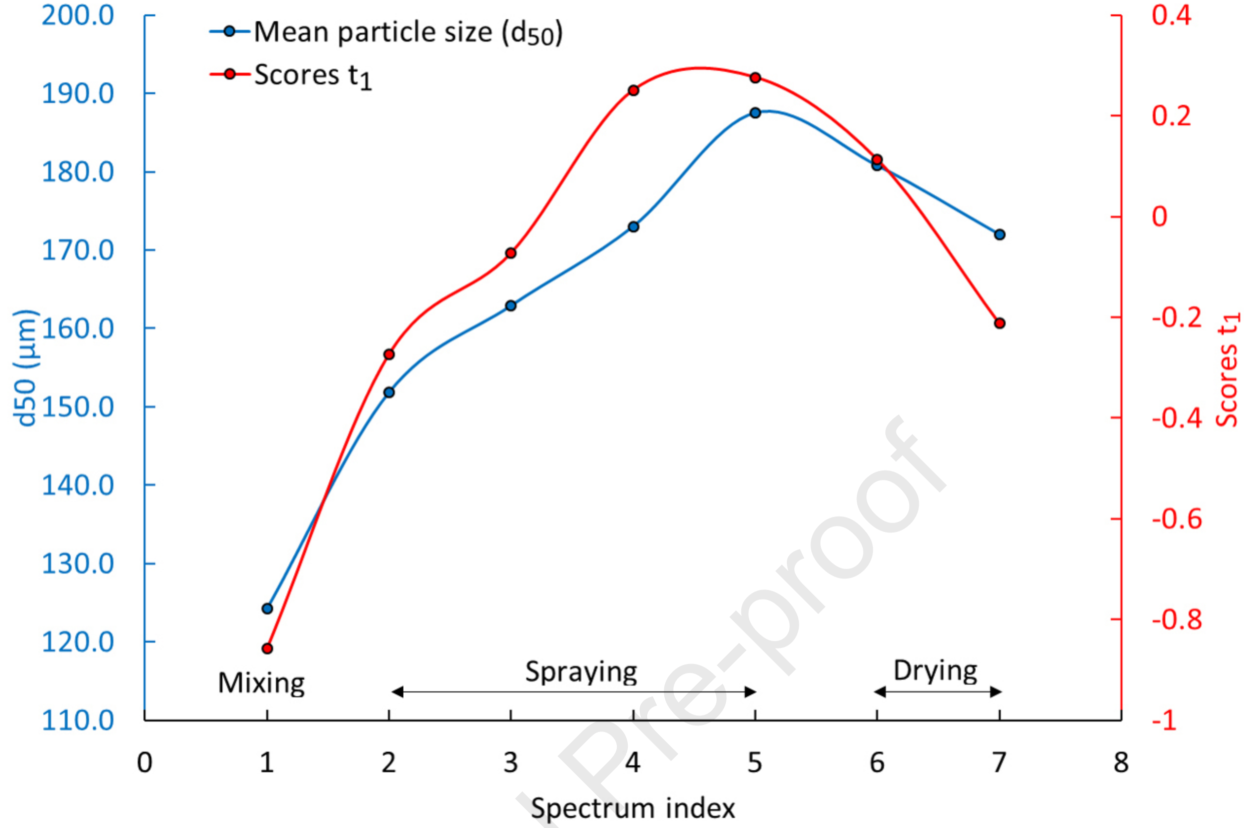

Mean particle size (d_{50})
Scores t_1
d50 (µm)
Scores t_1
200.0
190.0
180.0
170.0
160.0
150.0
140.0
130.0
120.0
110.0
0.4
0.2
0
-0.2
-0.4
-0.6
-0.8
-1
Mixing
Spraying
Drying
0
1
2
3
4
5
6
7
8
Spectrum index

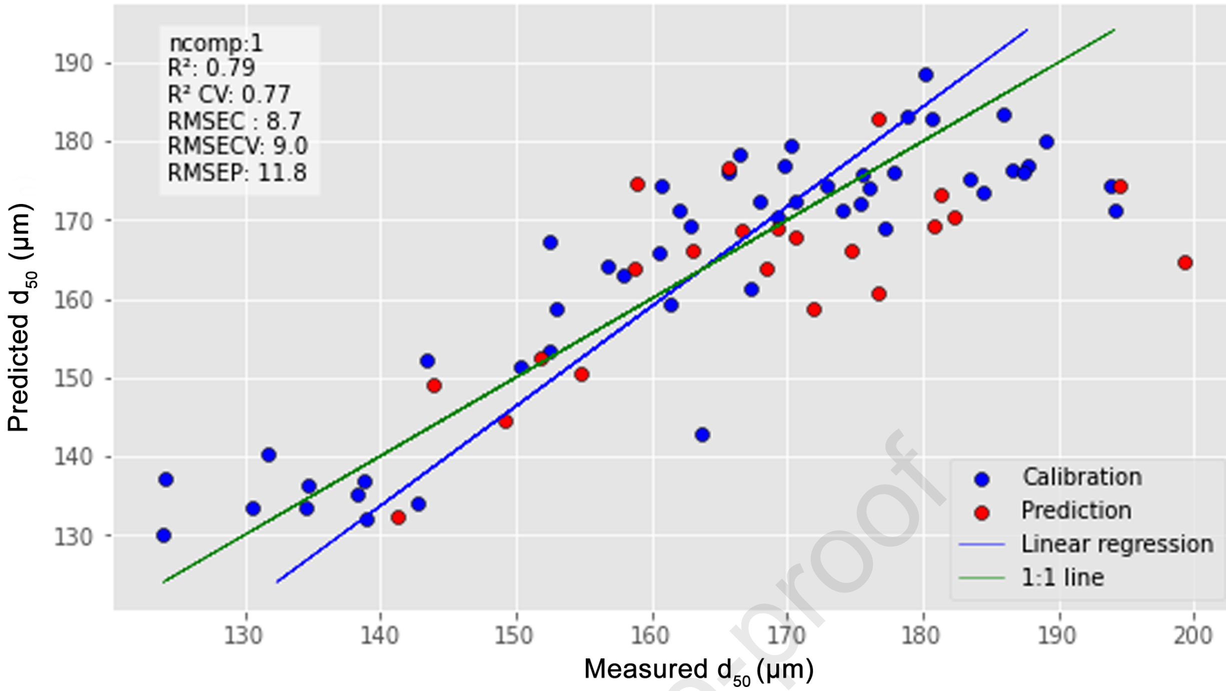
ncomp:1
R²: 0.79
R² CV: 0.77
RMSEC : 8.7
RMSECV: 9.0
RMSEP: 11.8
Calibration
Prediction
Linear regression
1:1 line
Predicted d50 (µm)
Measured d50 (µm)
130
140
150
160
170
180
190
200

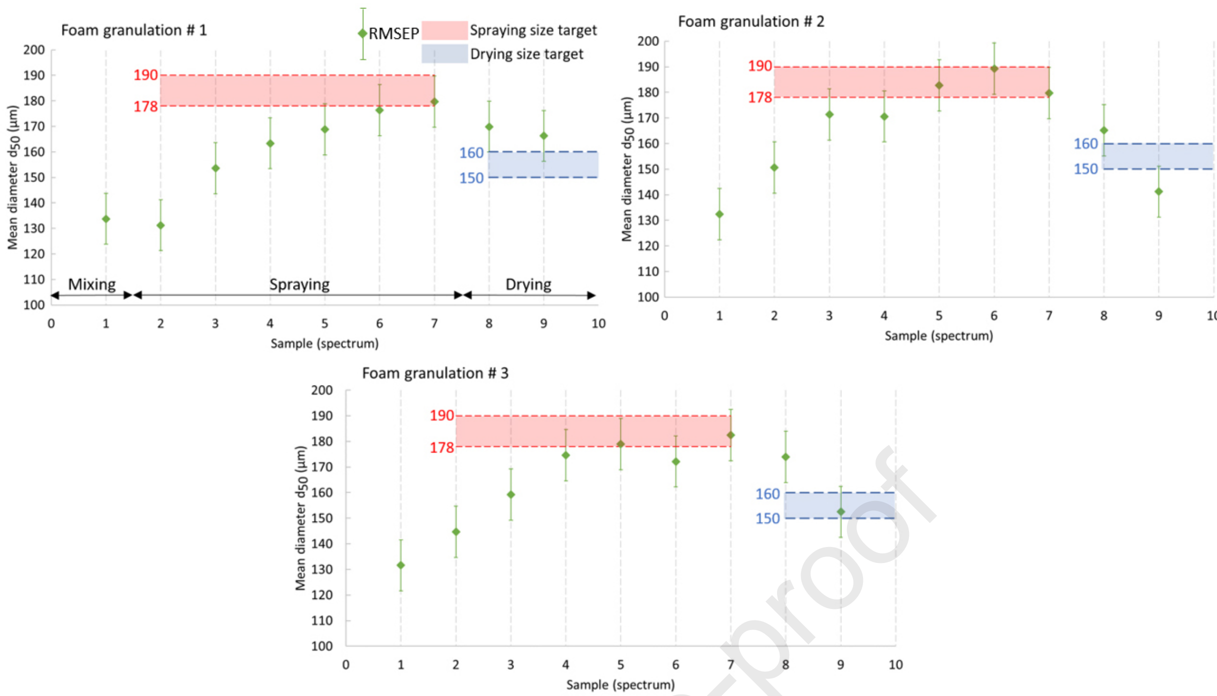

Foam granulation # 1
RMSEP
Spraying size target
Drying size target
190
178
160
150
Mixing
Spraying
Drying
Mean diameter d50 (µm)
Sample (spectrum)
Foam granulation # 2
190
178
160
150
Mean diameter d50 (µm)
Sample (spectrum)
Foam granulation # 3
190
178
160
150
Mean diameter d50 (µm)
Sample (spectrum)

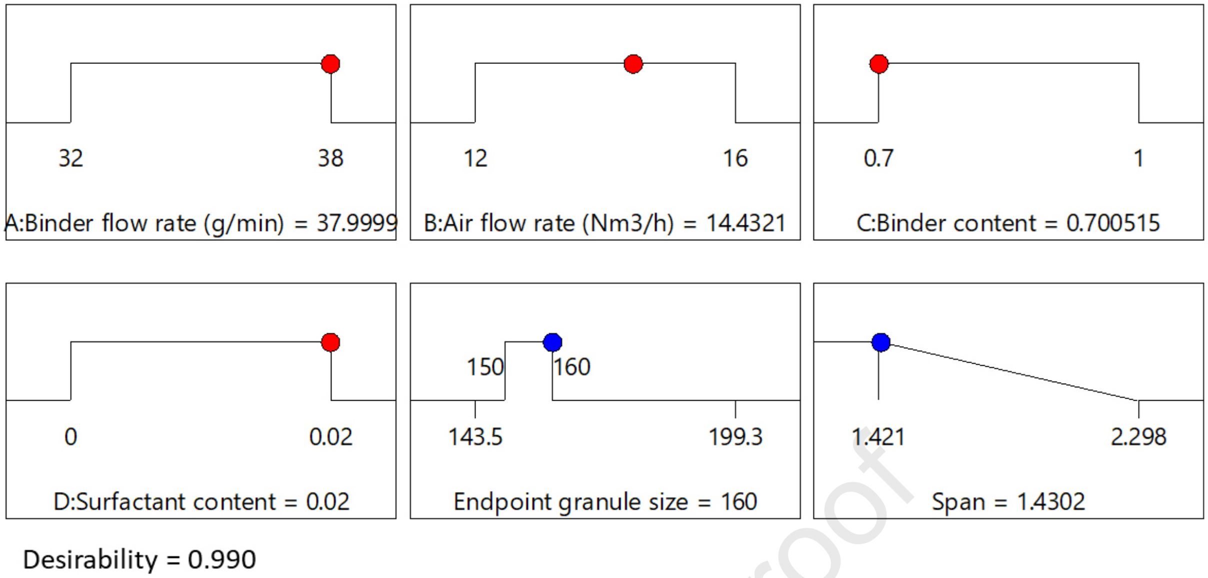
32
38
A:Binder flow rate (g/min) = 37.9999
12
16
B:Air flow rate (Nm3/h) = 14.4321
0.7
1
C:Binder content = 0.700515
0
0.02
D:Surfactant content = 0.02
150
160
143.5
199.3
Endpoint granule size = 160
1.421
2.298
Span = 1.4302
Desirability = 0.990

Predicting granule size via in-line NIR spectroscopy during fluidized bed foam granulation and drying

Romain Kersaudy[a], Maroua Rouabah[a*], Abdoulah Ly[b], Inès Esma Achouri[a], Ryan Gosselin[a], Nicolas Abatzoglou[a]

Highlights

- In-line monitoring of fluidized bed foam granulations via NIR spectroscopy.
- Partial least squares regression model built to predict mean granule diameter.
- Model predictions used with batch statistical process control to track granule size.

Declaration of Interest Statement

☒ The authors declare that they have no known competing financial interests or personal relationships that could have appeared to influence the work reported in this paper.

☐ The author is an Editorial Board Member/Editor-in-Chief/Associate Editor/Guest Editor for this journal and was not involved in the editorial review or the decision to publish this article.

☐ The authors declare the following financial interests/personal relationships which may be considered as potential competing interests: